Surfaces Presenting α-Phenyl Mannoside Derivatives Enable Formation of Stable, High Coverage, Non-pathogenic Escherichia coli Biofilms against Pathogen Colonization

Journal:	*Biomaterials Science*
Manuscript ID:	BM-ART-03-2015-000076.R1
Article Type:	Paper
Date Submitted by the Author:	09-Apr-2015

Complete List of Authors:	Zhu, Zhiling; University of Houston, Chemistry Wang, Jun; University of Houston, Chemistry Lopez, Analette; University of Houston, Chemistry Yu, Fei; University of Houston, Chemistry Huang, Yongkai; University of Houston, Chemistry Kumar, Amit; University of Houston, Chemistry Li, Siheng; University of Houston, Chemistry Zhang, Li Juan; South China University of Technology, School of chemistry and chemical engineering Cai, Chengzhi; University of Houston, Chemistry

Biomaterials Science

RSCPublishing

PAPER

Surfaces Presenting α-Phenyl Mannoside Derivatives Enable Formation of Stable, High Coverage, Non-pathogenic *Escherichia coli* Biofilms against Pathogen Colonization†

Cite this: DOI: 10.1039/xoxxoooooox

Received ooth January 2012,
Accepted ooth January 2012

DOI: 10.1039/xoxxoooooox

www.rsc.org/

Zhiling Zhu,[‡a] Jun Wang,[‡a] Analette I. Lopez,[‡a] Fei Yu,[a] Yongkai Huang,[a] Amit Kumar,[a] Siheng Li,[a] Lijuan Zhang[b] and Chengzhi Cai*[a]

Prevention of pathogenic colonization on medical devices over a long period of time remains a great challenge, especially in a high-nutrient environment that accelerates production of biomass leading to biofouling of the device. Since biofouling and the subsequent pathogen colonization is eventually inevitable, a new strategy using non-pathogenic bacteria as living guards against pathogenic colonization on medical devices has attracted increasing interest. Crucial to the success of this strategy is to pre-establish a high coverage and stable biofilm of benign bacteria on the surface. Silicone elastomers are one of the most widely used materials in biomedical devices. In this work, we modified silicone surfaces to promote formation of high coverage and stable biofilms by a non-pathogenic *Escherichia coli* strain 83972 with type 1 fimbriae (*fim*+) to interfere the colonization of an aggressive biofilm-forming, uropathogenic *Enterococcus faecalis*. Although it is well known that mannoside surfaces promote the initial adherence of *fim*+ *E. coli* through binding to the FimH receptor at the tip of the type 1 fimbriae, it is not clear whether the fast initial adherence could lead to a high coverage and stable protective biofilm. To explore the role of mannoside ligands, we synthesized a series of alkyl and aryl mannosides varied in structure and immobilized them on silicone surfaces pre-coated with poly(amidoamine) (PAMAM) dendrimer. We found that stable and densely packed benign *E. coli* biofilms were formed on the surfaces presenting biphenyl mannoside with the highest initial adherence of *fim*+ *E. coli*. These non-pathogenic biofilms prevented the colonization of *E. faecalis* for 11 days at a high concentration (10^8 CFU mL^{-1}, 100,000 times above the diagnostic threshold for urinary tract infection) in the nutrient-rich Lysogeny Broth (LB) media. The result shows a correlation among the initial adherence of *fim*+ *E. coli* 83972, the coverage and long-term stability of the resultant biofilms, as well as their efficiency for preventing the pathogen colonization.

Introduction

Adherence of pathogenic bacteria and their subsequent formation of biofilms on implantable devices is the leading cause of millions of healthcare-acquired infections, particularly catheter-associated urinary tract infections (CAUTI).[1-7] To prevent pathogenic colonization, hydrogel-, antibiotics- or silver-coated urinary catheters have come into clinical use, but studies indicated that they were ineffective or could only delay the onset of bacteriuria by <1 week.[7-11] A possible reason is that the pathogens grow rapidly in the high-nutrient environment, generating a large amount of biomass that fouls the coated surface.[8, 12] This and other related problems have driven extensive research on the development of new generation, "smart" antimicrobial or antifouling coatings.[7, 13-27] While great progress has been made in this line, the strong demand calls for exploration of alternative strategies. We have been exploring an alternative non-antibiotic strategy to prevent CAUTI based on bacterial interference,[2, 7, 28-30] in which non-pathogenic (benign) bacteria are used to form a biofilm that serves as a live, protective barrier against pathogen adhesion.[31-34] We hypothesize that the success of this strategy is critically dependent upon the coverage and stability of the benign biofilm on the material. To test this hypothesis, we have recently

developed an efficient method for tethering the mannoside **Man** (Fig. 1) onto polydimethylsiloxane (PDMS), a type of silicone polymers that are widely used in biomedical devices including silicone urinary catheters.[31] The mannoside-modified surfaces enhanced the ability of non-pathogenic *E. coli* 83972[2, 7, 34-38] with type 1 fimbriae (*fim*+), referred to as *fim*+ *E. coli* 83972, to form biofilms. *E. coli* 83972 has been used in many clinical trials in humans as an effective agent for bacterial interference against CAUTI.[2, 7, 39] We showed that the *fim*+ *E. coli* 83972 biofilms formed on the **Man**-presenting PDMS surfaces blocked the colonization of uropathogenic *E. faecalis* in a high-nutrient environment (lysogeny broth) for 3 days,[31] but the efficiency dropped rapidly for 5 days. Significant improvement would require substantial increase of the coverage and long-term stability of the *fim*+ *E. coli* 83972 biofilms.

Immobilized mannoside ligands are known to enhance the initial adherence of bacteria with type 1 fimbriae by interaction with the FimH receptor at the tip of the fimbriae.[40-44] However, since most reports have provided only the short-term (30 min) adherence data,[42, 43] it is unknown whether or not the initial fast bacterial adherence would subsequently result in a high coverage and stable biofilm on the mannoside-presenting surfaces.[45, 46] In fact, it has been reported that the fast initial bacterial adhesion on surfaces without specific ligand-receptor interactions does not correlate with the stability and coverage of the final biofilms.[47-51]

To understand the correlation among initial bacterial adherence, and biofilm coverage and long-term stability on various mannoside surfaces as well as the performance of the resultant biofilms on bacterial interference, in this work we studied the biofilm formation of *fim*+ *E. coli* 83972 on PDMS surfaces modified with a series of mannoside ligands with varied affinities to FimH receptors. We found a correlation among the initial adherence of *fim*+ *E. coli* 83972, and the coverage and long-term stability of the resultant biofilms, as well as the bacterial interference against pathogenic colonization. The surfaces presenting the biphenyl mannoside **BiPh-Man** (Fig. 1) had the highest initial adherence of *fim*+ *E. coli* 83972, and exhibited a significant improvement on the biofilm coverage and stability compared to the mannoside **Man**. Remarkably, these non-pathogenic biofilms blocked the colonization of *E. faecalis* at a high concentration (10^8 CFU mL^{-1}, 100,000 times above the diagnostic threshold for urinary tract infection) for 11 days in LB, a significant improvement over our previous system.[31, 52]

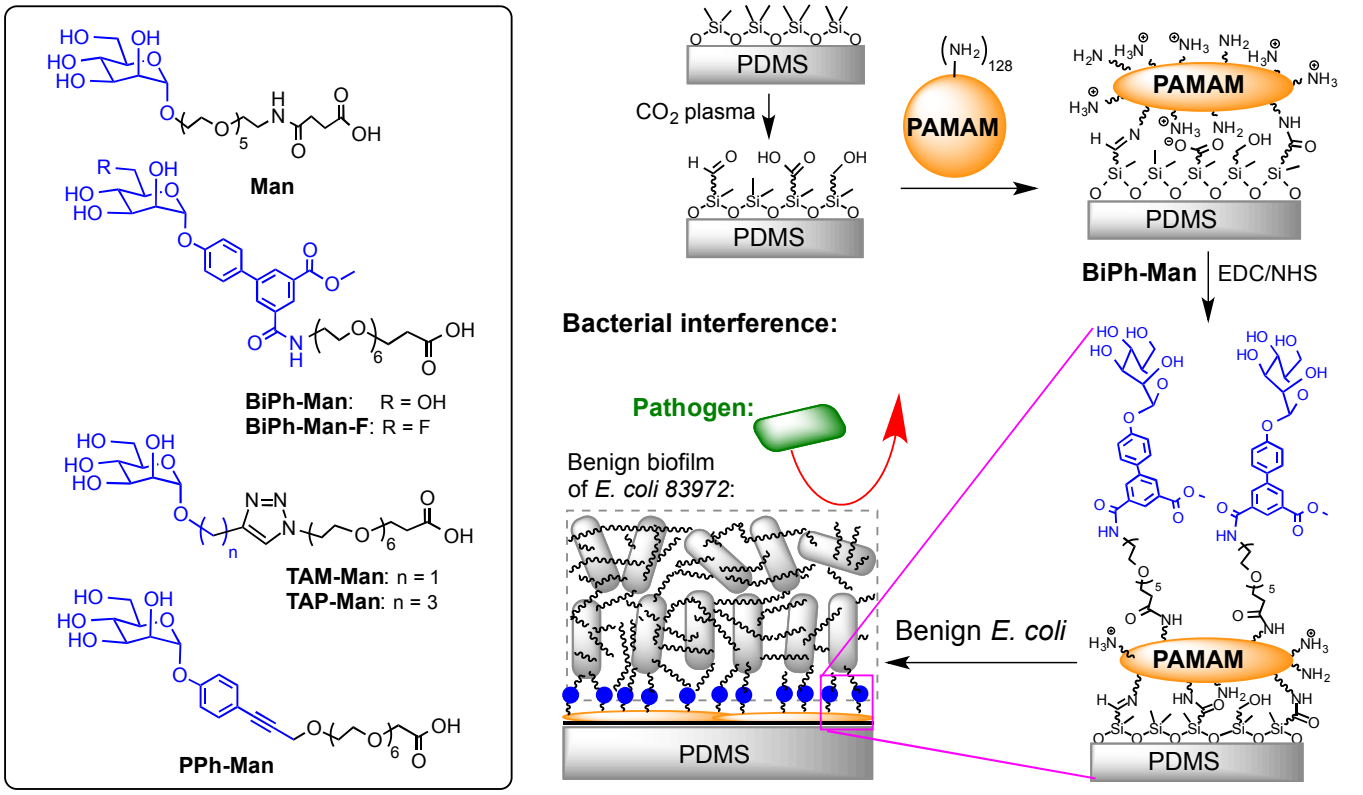

Fig. 1 Molecular structure of the mannosides with various glycosidic linkages, and illustration of benign *fim*+ *E. coli* 83972 biofilm formed on surface presenting the biphenylmannoside ligands (**BiPh-Man**) tethered on a PAMAM dendrimer platform readily prepared[31] on silicone to prevent uropathogenic colonization.

Experimental

Synthesis of mannosides

The detailed synthesis, purification and characterization of mannosides are given in ESI†.

Preparation of PDMS substrates

The silicone (PDMS) substrates were prepared according to our previously reported method with slight modifications.[31] Briefly, a 10:1 ratio of PDMS base and curing agent (SYLGARD 184

Silicone Elastomer Kit, Dow Corning) were mixed thoroughly and allowed to stand until no bubbles were detected in the mixture. The mixture was poured to a clean silicon wafer and pressed against a thin film of octadecyltrichlorosilane (OTS) (Sigma Aldrich) pre-formed on another silicon wafer. The mixture was cured at 110 °C overnight. Finally, the OTS-modified silicon wafer was peeled off to give a flat PDMS thin layer on the silicon wafer that was directly used in succeeding experiments.

PAMAM modification of PDMS surfaces

The surface modification of PDMS substrates with PAMAM was described in our previously report.[31] Briefly, the PDMS substrates were treated with CO_2 plasma using a Harrick plasma cleaner (Model PDC-32G, 100 W) with low power setting (6.8 W) for 45 s. The resultant oxidized PDMS were immediately immersed in a solution of generation 5 poly(amidoamine) dendrimer (G5 PAMAM, Dendritech Inc., Midland, MI) in phosphate buffered saline (PBS, 1 mg/mL) for 1 h. The PAMAM-modified surfaces were obtained after washing with Milli-Q water and drying with a flow of nitrogen.

Attachment of mannosides

A PAMAM-modified substrate was immersed in a solution containing 3 mM of each mannoside derivative (alkynylphenyl-mannoside **PPh-Man**, biphenyl-mannoside **BiPh-Man**, triazolylmethyl-mannoside **TAM-Man**, triazolylpropyl-mannoside **TAP-Man**, OEG mannoside **Man** and fluorinated-mannoside **BiPh-Man-F**, see Fig. 1), 60 mM of 1-ethyl-3-(3-dimethylaminopropyl) carbodiimide hydrochloride (EDC) and 30 mM *N*-hydroxysuccinimide (NHS) in Milli-Q water for 2 h. The surfaces were washed with Milli-Q water copiously and dried with a flow of nitrogen.

Characterization of mannoside-presenting surfaces

*Preparation of the standard for measurement of the surface density of **BiPh-Man-F***. Gold films coated on silicon wafers were initially treated with hydrogen plasma for 20 s followed by immediate immersion in a 2 mM solution of 14,14,14-trifluorotetradecane-1-thiol ($CF_3(CH_2)_{13}SH$) in absolute ethanol.[53] After 48 h, the films were washed with absolute ethanol, and dried with a flow of nitrogen to provide a self-assembled monolayer (SAM) of $CF_3(CH_2)_{13}SH$ on Au(111) surface.

X-ray photoelectron spectroscopy (XPS). A PHI 5700 X-ray photoelectron spectrometer was equipped with a monochromatic Al Kα X-ray source ($h\nu$ = 1486.7 eV) incident at 90° relative to the axis of a hemispherical energy analyzer. The spectrometer was operated both at high and low resolutions with pass energies of 23.5 eV and 187.85 eV, respectively, a photoelectron taken off angle of 45° from the surface, and an analyzer spot diameter of 1.1 mm. High resolution spectra were obtained for photoelectrons emitted from C1s, O1s, Si2p, N1s and F1s for the mannose surfaces, and Au4f and S2p for the fluorinated alkyl SAM standard. All spectra were collected at room temperature with a base pressure of 1×10^{-8} mbar. Electron binding energies were calibrated with respect to the Si2p line at 102.5 eV. A PHI Multipak software (Version 5.0A) was used for all data processing. The high resolution data were analyzed first by background subtraction using the Shirley routine and a subsequent non-linear fitting to the mixed Gaussian-Lorentzian functions. Atomic compositions were derived from the high-resolution scans. Peak areas were obtained after subtraction of the integrated baseline and corrected for sensitivity factors.

*Measurement of the surface density of **BiPh-Man-F***. The F1s XPS of the surfaces presenting **BiPh-Man-F** was measured together with the SAM of $CF_3(CH_2)_{13}SH$ on Au(111) as the reference. The F1s peak areas for the **BiPh-Man-F** and the CF_3-terminated SAM surface were $A_{F\text{-}Mannoside} = 668 \pm 33$ and $A_{F\text{-}SAM} = 29364 \pm 1170$, respectively. The numbers of fluorine atoms on the SAM and mannoside surfaces are $N_{F\text{-}SAM} = 3$ and $N_{F\text{-}Mannoside} = 1$, respectively. Using the density of the SAM on Au(111) as the standard, which is $D_{F\text{-}SAM} = 4.6 \times 10^{14}$ molecules/cm^2,[54] the fluorine coverage (7.9 ± 1.9)% and density ($(3.6 \pm 0.9) \times 10^{13}$ molecules/cm^2) of the F-mannoside were calculated with the following equations (1) and (2). The mean ± standard deviation was obtained from measurements of 6 samples presenting **BiPh-Man-F**.

$$\%\ \text{Fluorine}_{\text{F-mannoside}} = \frac{A_{\text{F-mannoside}}}{A_{\text{F-SAM}}} \times \frac{N_{\text{F-SAM}}}{N_{\text{F-mannoside}}} \times 100\% \quad (1)$$

$$D_{\text{F-mannoside}} = \%\ \text{Fluorine}_{\text{F-mannoside}} \times D_{\text{F-SAM}} \quad (2)$$

Contact-angle goniometry. Static water contact angles were measured with a KSV CAM 200 (KSV NIMA, Espoo, Finland) optical contact angle goniometer. At least three measurements were collected for each sample and data was presented as the mean ± standard deviation.

Bacterial strains

Both the *Escherichia coli* 83972 expressing type 1 fimbriae (*fim*+ *E. coli* 83972, strain HU2545)[35] and the challenge pathogenic bacteria, *Enterococcus faecalis* 210, were provided by Dr. Barbara W. Trautner (Baylor College of Medicine). This strain of *E. faecalis* was transformed with pMB158GFP to express green fluorescence protein (GFP) that can be observed by fluorescence microscopy. The protocol for bacterial preparation involved inoculation of a single colony from the bacterial plates into 50 mL of Lysogeny Broth (BD, Franklin Lakes, NJ) media containing appropriate antibiotics (20 μg/mL chloramphenicol (Sigma Aldrich) and 4 μg/mL tetracycline (Sigma Aldrich) for *fim*+ *E. coli* 83972 and *E. faecalis* 210, respectively). The optical density at 600 nm ($[OD]_{600}$) was adjusted to 0.25 for each bacterial culture after the overnight static incubation at 37 ºC, corresponding to a bacterial concentration of ~10^8 CFU mL^{-1}.

Adherence assay of *fim*+ *E. coli* 83972

A modified bacterial adherence assay was performed to evaluate the ability of *fim*+ *E. coli* 83972 to attach to different mannoside and control (PDMS and PAMAM) surfaces. Each sample surface was placed in a separate well of a 24-well plate and inoculated with 1 mL of 10^8 CFU mL^{-1} ($[OD]_{600} = 0.25$) of *fim*+ *E. coli* 83972. Chloramphenicol antibiotic (20 μg/mL) (Sigma Aldrich) was added. The substrates were incubated with the bacterial culture for 30 min or 48 h under static conditions at 37 ºC. After incubation, the surfaces were rinsed by immersing in PBS in a culture plate and gently shaking the plate back-and-forth three times by hand. This gentle rinsing step was repeated two more times to remove loosely attached

bacteria prior to quantification with microscopy imaging or plate counting.

Bacterial interference assay

Our previously reported assay was used with slight modifications.[31] Thus, the samples were placed in separate wells of a 24-well plate containing 1 mL of *fim*+ *E. coli* 83972 suspension (10^8 CFU mL^{-1}) in LB containing chloramphenicol antibiotics (20 μg/mL). The samples were incubated for 48 h at 37 ºC without shaking for biofilm formation on the surfaces. The samples were immediately transferred to 1 mL of fresh LB media (without antibiotics), which has been inoculated with a bacterial suspension of *E. faecalis* 210 (10^8 CFU mL^{-1}, $[OD]_{600}$ = 0.25), then incubated for 24 h at 37 ºC under static conditions. The media was replaced by a fresh bacterial suspension of *E. faecalis* 210 (10^8 CFU mL^{-1}, $[OD]_{600}$ = 0.25) every 24 h to a total of 5 and 11 days of continuous challenge by the pathogen. The surfaces were then immersed in PBS solution in a culture plate and the plate was gently shaken by hand in three back-and-forth motions on top of a desk. This gentle washing step was repeated two more times *to remove only the loosely attached bacteria* prior to quantification by imaging or plating. As a control, the corresponding mannoside surfaces without pre-treatment with *fim*+ *E. coli* 83972 were subjected to the above treatment with *E. faecalis* 210.

Microscopy imaging and quantification

For the bacterial adherence assay, the images were obtained using a 40× objective and reflected bright-field in a Nikon 80i Microscope with a CoolSnap HQ2 camera (Photometrics, Tucson, AZ). For the bacterial interference assay, *E. faecalis* 210 expressing GFP (λ_{em} = 535 nm) was differentiated from the non-fluorescent *fim*+ *E. coli* 83972 by fluorescence microscopy with a FITC filter. NIS Elements software (Version 3.0, Nikon Instruments, Melville, NY) and ImageJ software (Version 1.48, NIH) were used for image acquisition and analysis. First, the *fim*+ *E. coli* 83972 on the image was selected by adjusting the color threshold (Color space: HSB). The standing up bacteria that appeared like a black dot could also be selected by the same method. After the selection of *fim*+ *E. coli* 83972 on the images, the % coverage of *fim*+ *E. coli* 83972 was obtained. For the biofilms challenged by the *E. faecalis* 210 expressing GFP, the coverage by all bacteria on a bright-field image was obtained, followed by the coverage by the green *E. faecalis* in FITC channel over the same area. The coverage by *fim*+ *E. coli* 83972 was then obtained as the total coverage subtracting the *E. faecalis* coverage. Note that the possible presence of *fim*+ *E. coli* 83972 under *E. faecalis* 210 was ignored, which would lead to an underestimate of the coverage of *fim*+ *E. coli* 83972. Each data point expressed as mean ± standard deviation was obtained from 10 images taken on random locations of the sample and 3 experiments were repeated.

Z-series acquisition (Z-scan)

Z-scan (step: 1.5 μm, range: 25 μm) images were obtained with a 40× objective in reflected bright-field on the *fim*+ *E. coli* 83972 biofilm formed on a **BiPh-Man** surface after 48 hour of incubation. A CoolSnap HQ2 camera (Photometrics, Tucson, AZ) and NIS Elements software (Version 3.0, Nikon Instruments, Melville, NY) were used for image acquisition and analysis.

Quantification of bacterial interference by plate counting

The antibiotic resistance of *E. faecalis* 210 and *fim*+ *E. coli* 83972 was first tested for selective culture of the pathogen on agar plate. Luria Bertani agar (BD, Franklin Lakes, NJ) with chloramphenicol (20 μg/mL, Sigma), tetracycline (4 μg/mL, Sigma), ampicillin (100 μg/mL, Sigma) or carbenicillin (100 μg/mL, Teknova) were tested, and agar without any antibiotics was used as control. Culture of *E. faecalis* 210 or *fim*+ *E. coli* 83972 was prepared as mentioned above, and centrifuged at 5000 rpm for 10 min and then washed with PBS. The pellet was suspended in PBS and adjusted to $[OD]_{600}$ = 0.25, and diluted by factors of 10^2, 10^4, 10^6 and 10^8. Each diluted suspension (10 μL) was plated in duplicates on LB agar with the above antibiotics. The plates were incubated at 37 ºC and the bacterial colonies formed were counted after 24 h and expressed as colony forming unit per mL (CFU mL^{-1}). The results showed that *E. faecalis* 210 could only survive on agar without antibiotics (CFU = 2.0×10^8) or with tetracycline (CFU = 1.9×10^8), while *fim*+ *E. coli* 83972 could only survive on agar without antibiotics (CFU = 2.5×10^8) or with chloramphenicol (CFU = 2.0×10^8), but not on agar with tetracycline (CFU < 10^2). Hence, tetracycline was chosen for the following selective culture of *E. faecalis* 210.

We mixed *fim*+ *E. coli* 83972 and *E. faecalis* 210 with different ratio as 10^6 : 1, 10^4 : 1, 10^2 : 1 and 1:1 to test whether or not *fim*+ *E. coli* 83972 would influence the growth of *E. faecalis* 210 on agar in the presence of tetracycline. Thus, the mixed suspension was diluted by factors of 10^1, 10^2, 10^4, 10^6 and plated in duplicates on LB agar with tetracycline (4 μg/mL), and *E. faecalis* 210 suspension without *fim*+ *E. coli* 83972 was used as control. The colonies were counted after 24 h incubation. The results showed that colony-forming unit on the agar with tetracycline for the mixture of *fim*+ *E. coli* 83972 and *E. faecalis* 210 with the ratio of 10^6 : 1 (5.1×10^7), 10^4 : 1 (5.2×10^7), 10^2 : 1 (4.5×10^7) and 1:1 (4.7×10^7) was close to the control group (4.6×10^7). Therefore, this protocol can be used to selectively count viable *E. faecalis* 210 in the presence of a high concentration of *fim*+ *E. coli* 83972.

To quantify the bacteria on the surface, at the end of the 5-day bacterial interference, the samples following the final rinse with PBS were transferred to 1 mL solution of 0.01% sodium dodecyl sulfate (SDS), and sonicated for 10 min followed by vortexing for additional 1.5 min. Serial dilutions from the sonicated bacterial suspension (1, 10^{-2}, 10^{-4}, 10^{-6}, 10^{-8}) were prepared and 10 μL of each dilution was plated in duplicates on LB agar with tetracycline (4 μg/mL). The colonies formed after 24 h incubation at 37 °C were then counted. The viability of *E. coli* 83972 and *E. faecalis* at the relevant concentration after subjected to this condition did not change. Verification can be found in Fig. S3 and S4, ESI†.

Results and Discussion

As illustrated in Fig. 1, the α-D-mannoside ligands are attached via an oligo(ethylene glycol)-COOH (OEG-COOH) chain to the 5th generation, NH_2-terminated poly(amidoamine) (G5-PAMAM) dendrimer molecules that are bound to the CO_2-plasma activated silicone surface as described in detail in our previous report.[31] For choosing the mannoside ligands, we focused on the monomannosides with varied glycosidic linkages rather than oligomannosides that generally require laborious synthesis while are not always effective in enhancing the binding affinity to FimH.[41] In fact, Barth *et al.* recently revealed that the initial adhesion of *E. coli* onto surfaces

presenting propyl mannosides was comparable to a variety of oligomannosides up to a 9-mer.[43] The glycosidic substituents of mannosides have been shown to substantially affect the binding with FimH in solution.[55-57] A high binding affinity is associated with certain hydrophobic groups, such as alkyl,[55] alkynylphenyl[56] and biphenyl.[57] Hence, we synthesized a series of mannosides including the biphenyl mannoside **BiPh-Man**, the triazolylalkyl mannosides **TAM-Man** and **TAP-Man** and the alkynylphenyl mannoside **PPh-Man**, tethering an OEG-COOH anchoring group. They all contain an aromatic ring and exhibit a variety of affinity to FimH.[55-57] The analogue **BiPh-Man-F** of the mannoside **BiPh-Man** with the 6-OH group replaced by a fluorine atom was used to test the specificity of the interactions with the bacteria, and more importantly also to allow quantification of the surface density of the mannosides by X-ray photoelectron spectroscopy (XPS, see below)

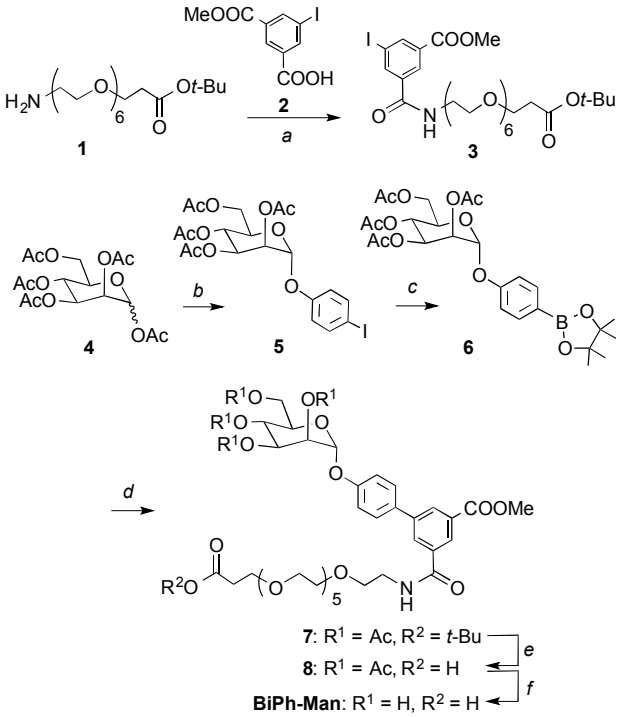

Scheme 1 Synthesis of **BiPh-Man**. Reagents and conditions: *a*) HBTU, diisopropylethylamine, CH_2Cl_2, rt, 15 h, 78%; *b*) Triflic acid, 4-iodophenol, CH_2Cl_2, 0ºC, 12 h, 78%; *c*) bis(pinacolato)diboron, $PdCl_2$(dppf), AcOK, DMSO, 80ºC, 10 h, 85%; *d*) CsF, $Pd(PPh_3)_4$, THF, 80ºC, 12 h, 81%; *e*) TFA, CH_2Cl_2, rt, 15 h, 99%; *f*) NaOMe, MeOH, rt, 12 h, 50%.

The syntheses of the mannosides were described in details in ESI†. As an example, Scheme 1 outlines the synthesis of the mannoside **BiPh-Man** with a biphenyl linkage, based on a convergent approach using Suzuki coupling to connect the two phenylene units. Thus, the bifunctional OEG derivative **1** was coupled with the iodo-benzenedicarboxylic acid monoester **2** in the presence of HBTU and DIPEA to provide the building block **3** in 78% yield. On the other hand, triflic acid mediated glycosylation of the pentaacetylmannoside **4** with 4-iodophenol gave exclusively the α-anomer of iodophenyl mannoside **5**.[56] Conversion of the iodide **5** to the boronic esters **6** was conducted with bis(pinacolato)diboron catalyzed by $PdCl_2$(dppf) in 85% yield. Suzuki coupling of **6** and **3** provided the biphenyl mannoside **7** in 81% yield. While the *t*-butyl group in **7** was readily removed by TFA, deacetylation of the resultant **8** with MeONa needed to be performed in anhydrous MeOH to furnish the desired biphenyl mannoside **BiPh-Man** in 50% yield over two steps.

The COOH-terminated mannosides were attached via amidation to the silicone (polydimethylsiloxane, PDMS) surfaces presenting amino-terminated PAMAM dendrimers prepared according to our previously reported method (Fig. 1).[31] Briefly, flat PDMS surfaces were treated with CO_2 plasma for 45 s, followed by 1 h immersion in a 1 mg/mL solution of G5 PAMAM dendrimer in PBS buffer. The PAMAM dendrimer was used to cross-link the oxidized PDMS polymers, leading to an excellent stability. Indeed, the resultant PAMAM platform was stable against desorption in PBS for 6 weeks.[31] The COOH-terminated mannosides were then attached to the PAMAM surfaces in the presence of EDC/NHS in Milli-Q water for 2 h.

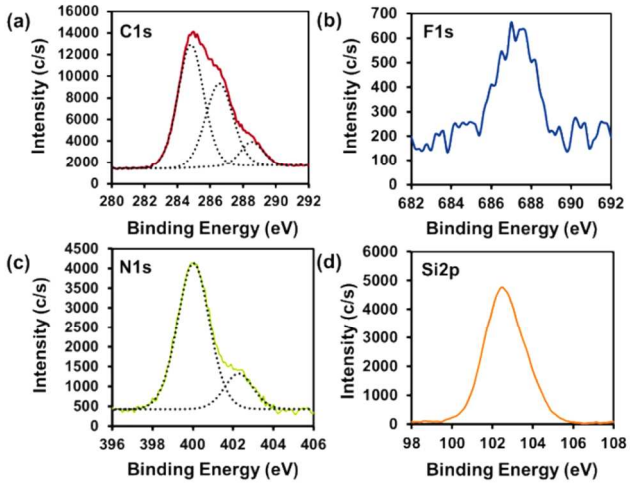

Fig. 2 XPS high resolution scans for a film derived from the fluorinated-mannoside **BiPh-Man-F**.

Table 1 Advancing (θ_a) and receding (θ_r) water contact angles of various mannoside, PAMAM and PDMS surfaces.

Surface	θ_a / º	θ_r / º
Man	51 ± 1	48 ± 1
BiPh-Man	58 ± 1	54 ± 0
BiPh-Man-F	60 ± 2	55 ± 1
TAM-Man	64 ± 1	61 ± 0
TAP-Man	59 ± 2	55 ± 2
PPh-Man	53 ± 2	49 ± 2
PAMAM	69 ± 3	66 ± 3
PDMS	117 ± 1	111 ± 3

Quantification of the density of the immobilized mannosides is challenging. Recently, Dhayal and Ratner developed a XPS C1s core level analysis method to quantify the glycosidic carbon atoms in trimannosides incorporated in mixed self-assembled monolayers (SAMs) on gold.[58] However, this method is not applicable to our system due to the extensive overlap of the C1s signals. To circumvent this difficulty, we synthesized the fluorinated-mannoside **BiPh-Man-F** as a close analogue of **BiPh-Man** (Fig. 1) and attached it to the PAMAM platform under identical conditions. Although the synthesis was tedious, taking 18 steps (ESI†), the presence of the F-atom in

BiPh-Man-F allowed us to quantify its density on the surface. Thus, the films derived from **BiPh-Man** showed the deconvoluted C1s peaks at 284.8 eV, 286.5 eV and 288.5 eV (Fig. 2a), assigned to the alkyl groups (C-C) from PAMAM and PDMS, C-O moieties in the mannoside and OEG chains and C-N in PAMAM, and C=O moieties in PAMAM, respectively. A F1s peak appeared at around 687 eV (Fig. 2b), confirming the attachment of **BiPh-Man-F**. The deconvoluted N1s peaks at 400.0 eV and 402.0 eV (Fig. 2c) can be attributed to the amino and amide moieties and the presence of NH_3^+ groups in PAMAM, respectively. The PDMS Si2p signal appeared at 102.5 eV (Fig. 2d). A fluorine density of $((3.6 \pm 0.9) \times 10^{13}$ molecules/cm^2 was derived from the F1s peak area using a self-assembled monolayer prepared from 14,14,14-trifluoro-tetradecane-1-thiol on gold with a known density as the reference. The attenuation of F1s signal due to the possible burying of some mannoside groups into the film was ignored, which would lead to an underestimate of the density. Assuming the same reaction yield of **BiPh-Man** and **BiPh-Man-F** with the amino surface, which should be a reasonable assumption since the only difference between the two molecules is the substituent at C(6) that is far from the reaction center (COOH), this density ($(3.6 \pm 0.9) \times 10^{13}$ molecules/cm^2) represents the density of mannoside derived from **BiPh-Man** on the PDMS surface. Similarly, the influence of the glycosidic linkage on the amidation reaction occurring at the end of the long OEG linker might be small. Hence the above density for **BiPh-Man-F** was probably typical for the other mannoside surfaces. The variation of glycosidic linkages did not substantially affect the surface energy, as indicated by a relatively small variation (<10º) of the advancing or receding water contact angles (Table 1). The small hysteresis (<5º) of the advancing and receding water contact angles suggested that the surfaces were relatively homogenous and flat.

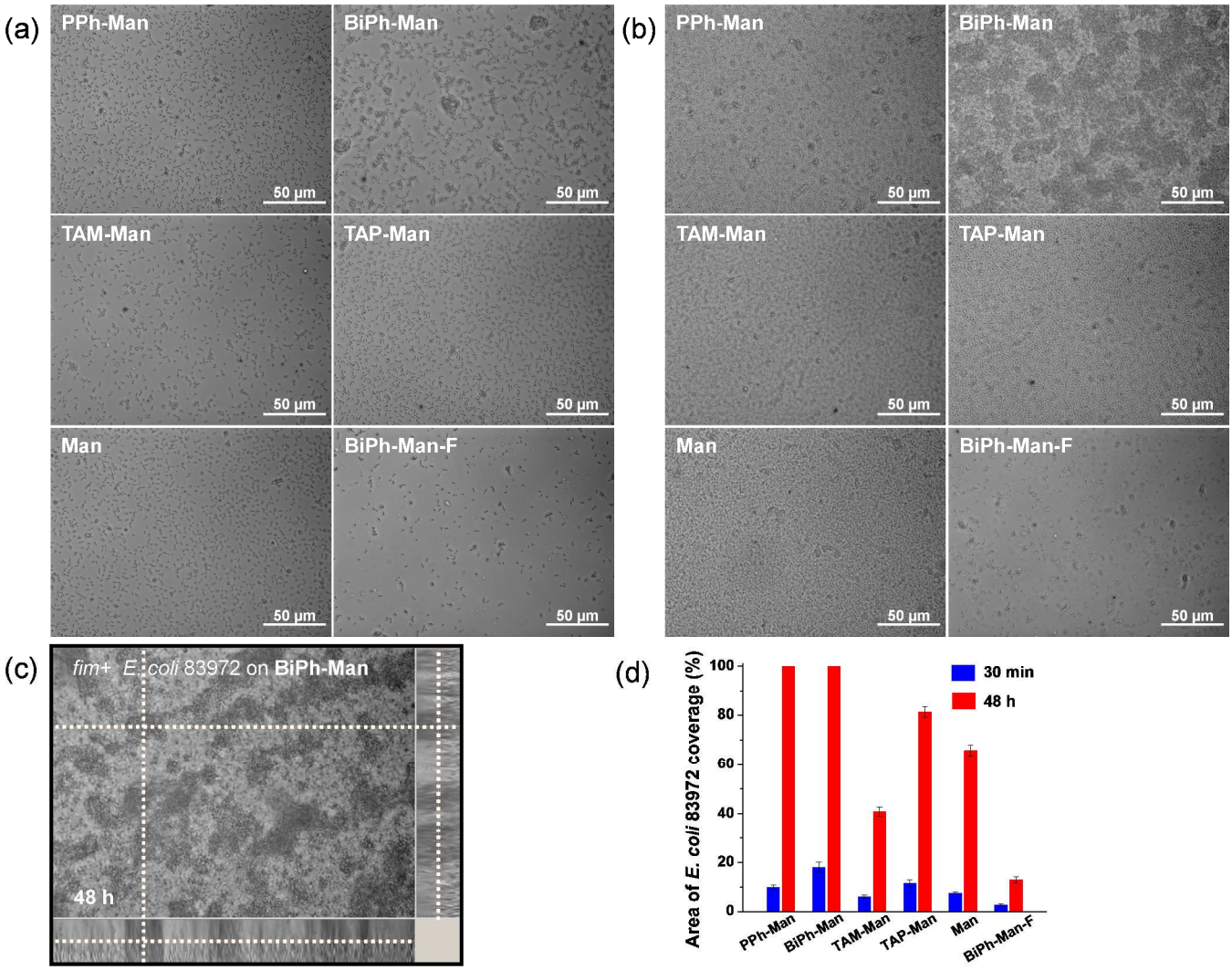

Fig. 3 Representative reflected bright-field images of the adhered *fim+ E. coli* 83972 after 30 min incubation (a) and the corresponding biofilm formed after 48 h (b, c) on the indicated mannoside surfaces. (c) A bright-field image at the middle of a biofilm of *fim+ E. coli* 83972 formed after 48 hour of incubation with z-scan images (step: 1.5 µm, range: 25 µm) on the right obtained across the vertical dot line and at the bottom obtained across the horizontal dot line, showing that the biofilm was about 20 µm thick, and fully covered the substrate surface. (d) Plot of the coverage of *fim+ E. coli* 83972 at 30 min and 48 h on various mannoside surfaces. Each image is representative of up to 10 images obtained on random locations at each surface and 3 experiments were repeated. More details can be seen by setting the view of the document to 500%. The images of *fim+ E. coli* 83972 on the control surfaces (PDMS and G5 PAMAM) are provided in Fig. S1 (ESI†).

Biomaterials Science RSCPublishing

PAPER

The adherence of the *fim*+ *E. coli* 83972 on the PDMS, PAMAM and mannoside-presenting surfaces was evaluated using a relatively short incubation time (30 min) to observe the initial attachment of the bacteria and 48 h incubation for biofilm formation. A suspension of *fim*+ *E. coli* 83972 at an initial concentration of 10^8 CFU mL^{-1} of the benign bacteria in LB was used to incubate the substrates at 37 °C. Reflected bright-field images (Fig. 3a) showed more bacteria adhered within 30 min on the **TAP-Man** surface than on the **TAM-Man** surface which was similar to the one derived from the OEG mannoside **Man**. This result indicated that the triazolyl moiety did not enhance the bacterial adherence, while the alkyl moiety directly attached to the glycosidic position did, in accordance with the report that longer alkyl chains increased the affinity to FimH.[55] The alkynylphenyl moiety promoted the bacterial adherence, in consistent with its large enhancement of the binding affinity of mannoside to FimH.[56] Among the mannosides tested, the biphenylmannoside **BiPh-Man** and alkynylphenylmannoside **PPh-Man** turned out to attract most *fim*+ *E. coli* 83972 onto the surface (Fig. 3d). The biphenyl moiety was recently shown to largely enhance the binding with FimH through a combination of the π-π interactions, hydrogen bonding and electrostatic interactions.[57] As expected, the analogous fluorinated biphenyl mannoside **BiPh-Man-F** surfaces attracted far less bacteria (Fig. 3). The result proves that the mannoside but not the biphenyl moiety was the primary binding site, although the binding was greatly enhanced by the secondary interactions with the biphenyl moiety.[59] Noteworthy, the wild type *E. coli* 83972 without fimbriae did not adhere to mannoside surfaces.[33, 60] supporting that the type 1 fimbriae on *fim*+ *E. coli* 83972 were crucial for the initial bacterial adherence.

How did the initial adherence of *fim*+ *E. coli* 83972 on the mannoside surfaces affect the subsequent biofilm coverage and stability? As shown in Fig. 3b and 3d, after 48 hours of incubation in culture of *fim*+ *E. coli* 83972, the apparent density of the bacteria attached on the mannoside surfaces decreased with the following order (Fig. 3d): **BiPh-Man** ≈ **PPh-Man** > **TAP-Man** > **Man** > **TAM-Man** > **BiPh-Man-F**. This order was similar to the one for initial adherences. In particular, thick biofilms were generated on the **BiPh-Man** surface as shown by the z-scan image (Fig. 3c).

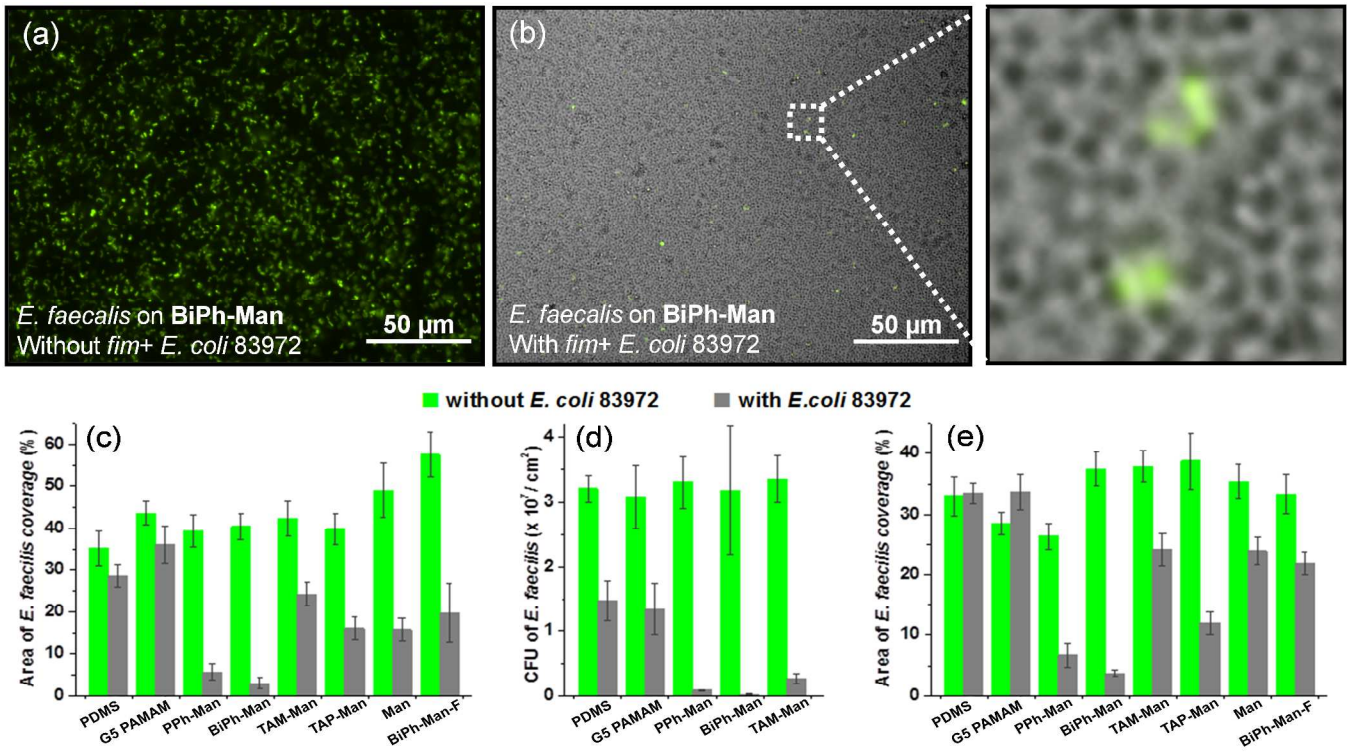

Fig. 4 Performance of bacterial interference against *E. faecalis* 210 adhesion onto biofilms of *E. coli* 83972 on various mannoside surfaces. (a): A fluorescence image of a biofilm of *E. faecalis* grown on a **BiPh-Man** surface without pre-treatment with the *fim*+ *E. coli* 83972 for 5 days. (b): An overlay of the fluorescence and reflected bright-field images of a densely packed biofilm of *fim*+ *E. coli* 83972 after 5 days incubation in 10^8 CFU mL^{-1} of the green fluorescent *E. faecalis*, and the amplified image showing few *E. faecalis* 210 attached on the surface. (c-e): Quantification of *E. faecalis* adhesion, after 5 days (c, d) and 11 days (e) of incubation in 10^8 CFU mL^{-1} of *E. faecalis* in LB, on the indicated surfaces with (gray) and without (green) a *fim*+ *E. coli* 83972 biofilm. The quantification was based on the coverage of the green-fluorescent *E. faecalis* (c, e), and the CFU counts (d) of the *E. faecalis* on the surfaces. The fluorescent coverage data for (c) and (e) were obtained in triplicate, in which fluorescence images

(*e.g.* Fig. S2, ESI†) were taken on 10 randomly chosen locations on each sample surface, and the images were processed with NIS Element software in a Nikon microscope and imageJ software to provide the mean coverage +/- standard deviation. The data represents an underestimate due to the presence of multilayer of *E. faecalis* outside the focal plane, especially for the thick *E. faecalis* films formed in the absence of *fim*+ *E. coli* 83972. The CFU counts of *E. faecalis* in (d) were obtained in triplicate by detaching the bacteria from the surface with sonication followed by selective plating in the presence of tetracycline (4 μg/mL) that selectively kills *fim*+ *E. coli* 83972. The values were expressed as mean +/- standard deviation. The error due to a low density of the *E. faecalis* adhered on the backside of the wafer was corrected by counting them with fluorescence imaging (triplicate on 10 random locations). The counting results showed the bacterial density was lower than 2.0×10^3 CFU cm^{-2} on the backside which was less than 1% of the *E. faecalis* on the front side even for the **BiPh-Man** surface.

Bacterial interference was then performed on the *fim*+ *E. coli* 83972 biofilms generated on various mannoside surfaces after 48 h incubation (Fig. 4). The samples were continuously challenged with fresh bacterial suspension (10^8 CFU mL^{-1}) of *E. faecalis* in LB media everyday for up to 11 days (note that this concentration is three orders of magnitude above the diagnostic threshold for urinary tract infection). We chose *E. faecalis* 210 as the challenge bacteria since it is an uropathogenic isolate with a strong ability to form biofilms.[61, 62] This strain of *E. faecalis* was transformed to express green fluorescence protein (GFP) that can be observed by fluorescence microscopy (Fig. 4a and 4b). After 5 days, the results clearly showed that the presence of *fim*+ *E. coli* 83972 reduced the adherence of *E. faecalis* on all surfaces modified with mannosides (Fig. 4c and 4d). The coverage of the *E. faecalis* on the mannoside surfaces pre-treated with *fim*+ *E. coli* 83972 (for 48 h) decreased with the following order of the glycosidic linker: **TAM-Man** > **BiPh-Man-F** > **TAP-Man** ≈ **Man** > **PPh-Man** > **BiPh-Man**, which is similar to the order for the initial adherence and the biofilm coverage of *fim*+ *E. coli* 83972 (after 48 h incubation).

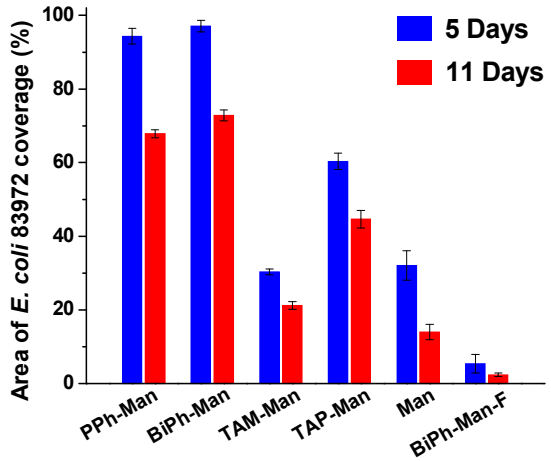

Fig. 5 Quantification of *fim*+ *E. coli* 83972 coverage after 5 days and 11 days of incubation in 10^8 CFU mL^{-1} of *E. faecalis* in LB. The coverage of *fim*+ *E. coli* 83972 was obtained by subtracting the coverage of *E. faecalis* on the green-fluorescent images from the total bacterial coverage of *E. faecalis* and *fim*+ *E. coli* 83972 on the reflected bright-field images. Note that the possible presence of *fim*+ *E. coli* 83972 under *E. Faecalis* 210 was ignored, which would lead to an underestimate of the coverage of *fim*+ *E. coli* 83972. The fluorescent and the reflected bright-field coverage data were obtained in triplicate, in which the images (Figure S2) were taken on 10 randomly chosen locations on each sample surface, and were processed with NIS Element software to provide the mean coverage +/- standard deviation.

Interestingly, after the above interference test for 5 days, the overlayer of *fim*+ *E. coli* 83972 on the **BiPh-Man** surface shown in Fig. 4b disappeared, but the *fim*+ *E. coli* 83972 biofilm remained densely packed as shown in Fig. 4b, in which few green fluorescent *E. faecalis* were found. In comparison, the surfaces without pre-treatment with *fim*+ *E. coli* 83972 were mostly covered with *E. faecalis* (Fig. 4a, 4c and 4d). As shown in Fig. 5, the *fim*+ *E. coli* 83972 biofilm coverage and stability after challenged by *E. faecalis* for 5 days was in the order of **Bi-Man** ≈ **PPh-Man** > **TAP-Man** > **TAM-Man** ≈ **Man** > **BiPh-Man-F**. This order was similar to the order of the initial adherence of *fim*+ *E. coli* 83972 and its biofilm coverage after 48 h growth on the mannoside surfaces.

In addition to the microscopy-based quantification, the more laborious plate counting of adhered *E. faecalis* on selected samples was performed to validate the above results. Specifically, we chose to count *E. faecalis* on *fim*+ *E. coli* 83972 biofilms grown on **BiPh-Man, PPh-Man** and **TAM-Man** by selective plating.[35] The bacteria were detached by sonication and vortex in 0.01 % sodium dodecyl sulfate (SDS) solution. As shown in Fig. 4c and 4d, both the microscopy quantitation based on *E. faecalis* coverage and selective plating gave the same trend.

After continuously challenged by *E. faecalis* for 11 days, as shown in Fig. 4e and Fig. S2 (ESI†), the biofilm of *fim*+ *E. coli* 83972 on the **BiPh-Man** and **PPh-Man** surfaces remained effective in fencing off *E. faecalis*. In contrast, all other mannoside surfaces have been colonized by *E. faecalis*. Remarkably, the *fim*+ *E. coli* 83972 biofilm still maintained a high coverage (~70%, Fig. 5) on the **BiPh-Man** and **PPh-Man** surfaces even after continuously challenged by *E. faecalis* at a high concentration (10^8 CFU mL^{-1}, culture changed everyday) for 11 days in LB media. As shown by Fig. 5, the orders of the *fim*+ *E. coli* 83972 biofilm coverage on the mannoside surfaces after being challenged by *E. faecalis* for 5 and 11 days were the same, which were similar to the order of their initial adherence and biofilm coverage. These orders were also the same for the performance of these biofilms on the bacterial interference against the colonization by *E. faecalis* after 11 days as shown by Fig. 4e.

Conclusions

In summary, we have demonstrated that the initial adherence of *fim*+ *E. coli* 83972 to the mannoside-modified surfaces qualitatively correlated to the coverage, stability and bacterial interference of the biofilms subsequently formed thereon. Overall, this work has shown the importance of specific mannoside-FimH interaction on enhancing the coverage and stability of the benign biofilms leading to excellent prolonged bacterial interference against the aggressive biofilm-forming pathogen *E. faecalis* in LB media. For potential applications in a clinical setting, further extensive research will be necessary to assess the safety of the bacterial strain and its biofilms on the silicone catheters for long-term use.

Acknowledgements

We acknowledge the use of *fim*+ *E. coli* 83972 and *E. faecalis* bacterial strains provided by Dr. Barbara W. Trautner at Baylor

College of Medicine, and the financial support by NSF DMR1207583 and NIH HD058985.

Notes and references

[a] 112 Fleming Building, Department of Chemistry, University of Houston, Houston, Texas, 77204, USA. E-mail: cai@uh.edu; Fax: +1-713-743-2709; Tel: +1-713-743-2710.
[b] School of Chemistry and Chemical Engineering, South China University of Technology, Guangzhou 510640, P R China.

† Electronic Supplementary Information (ESI) available for synthesis and characterization of the mannosides, imaging and plate counting of the bacteria. See DOI: 10.1039/b000000x/

‡ These authors contributed equally to this work.

1 A. Y. Peleg and D. C. Hooper, *N. Engl. J. Med.*, 2010, **362**, 1804-1813.
2 R. O. Darouiche and R. A. Hull, *Clin. Infect. Dis.*, 2012, **55**, 1400-1407.
3 R. Kolter and E. P. Greenberg, *Nature*, 2006, **441**, 300-302.
4 S. Noimark, C. W. Dunnill, M. Wilson and I. P. Parkin, *Chem. Soc. Rev.*, 2009, **38**, 3435-3448.
5 B. W. Trautner, R. L. Atmar, A. Hulstrom and R. O. Darouiche, *Arch. Phys. Med. Rehabil.*, 2004, **85**, 1886-1889.
6 S. M. Jacobsen, D. J. Stickler, H. L. T. Mobley and M. E. Shirtliff, *Clin. Microbiol. Rev.*, 2008, **21**, 26-59.
7 D. M. Siddiq and R. O. Darouiche, *Nat. Rev. Urol.*, 2012, **9**, 305-314.
8 D. G. Desai, K. S. Liao, M. E. Cevallos and B. W. Trautner, *J. Urol.*, 2010, **184**, 2565-2571.
9 R. Pickard, T. Lam, G. MacLennan, K. Starr, M. Kilonzo, G. McPherson, K. Gillies, A. McDonald, K. Walton, B. Buckley, C. Glazener, C. Boachie, J. Burr, J. Norrie, L. Vale, A. Grant and J. N'Dow, *Health Technol. Assess.*, 2012, **16**, 1-197.
10 R. C. L. Feneley, C. M. Kunin and D. J. Stickler, *Bju Int.*, 2012, **109**, 1746-1749.
11 K. A. Kazmierska, R. Thompson, N. Morris, A. Long and T. Ciach, *Urology*, 2010, **76**, 515.e15-515.e20.
12 J. A. Lichter, K. J. Van Vliet and M. F. Rubner, *Macromolecules*, 2009, **42**, 8573-8586.
13 S. Y. Wong, J. S. Moskowitz, J. Veselinovic, R. A. Rosario, K. Timachova, M. R. Blaisse, R. C. Fuller, A. M. Klibanov and P. T. Hammond, *J. Am. Chem. Soc.*, 2010, **132**, 17840-17848.
14 G. Cheng, H. Xue, G. Z. Li and S. Y. Jiang, *Langmuir*, 2010, **26**, 10425-10428.
15 S. Y. Hou, E. A. Burton, R. L. Wu, Y. Y. Luk and D. C. Ren, *Chem. Commun.*, 2009, 1207-1209.
16 J.-Y. Wach, S. Bonazzi and K. Gademann, *Angew. Chem. Int. Ed.*, 2008, **47**, 7123-7126.
17 I. C. S. Fernandez, H. C. van der Mei, S. Metzger, D. W. Grainger, A. F. Engelsman, M. R. Nejadnik and H. J. Busscher, *Acta Biomaterialia*, 2010, **6**, 1119-1124.
18 B. Cao, L. L. Li, Q. Tang and G. Cheng, *Biomaterials*, 2013, **34**, 7592-7600.
19 B. Fang, Y. Jiang, V. M. Rotello, K. Nusslein and M. M. Santore, *Acs Nano*, 2014, **8**, 1180-1190.
20 Z. Cao, L. Mi, J. Mendiola, J.-R. Ella-Menye, L. Zhang, H. Xue and S. Jiang, *Angew. Chem. Int. Ed.*, 2012, **51**, 2602-2605.
21 L. Mi and S. Jiang, *Angew. Chem. Int. Ed.*, 2014, **53**, 1746-1754.
22 C. Diaz Blanco, A. Ortner, R. Dimitrov, A. Navarro, E. Mendoza and T. Tzanov, *ACS Appl. Mater. Interfaces*, 2014, **6**, 11385-11393.
23 N. Hadjesfandiari, K. Yu, Y. Mei and J. N. Kizhakkedathu, *J. Mater. Chem. B*, 2014, **2**, 4968-4978.
24 I. Banerjee, R. C. Pangule and R. S. Kane, *Adv. Mater.*, 2011, **23**, 690-718.
25 S. Hou, C. Zhou, Z. Liu, A. W. Young, Z. Shi, D. Ren and N. R. Kallenbach, *Bioorg. Med. Chem. Lett.*, 2009, **19**, 5478-5481.
26 T. H. R. Niepa, J. L. Gilbert and D. Ren, *Biomaterials*, 2012, **33**, 7356-7365.
27 G. S. Shetye, N. Singh, X. Gao, D. Bandyopadhyay, A. Yan and Y.-Y. Luk, *MedChemComm*, 2013, **4**, 1079-1084.
28 M. Ventura, S. O'Flaherty, M. J. Claesson, F. Turroni, T. R. Klaenhammer, D. van Sinderen and P. W. O'Toole, *Nat. Rev. Microbiol.*, 2009, **7**, 61-U77.
29 M. Saxelin, S. Tynkkynen, T. Mattila-Sandholm and W. M. de Vos, *Curr. Opin. Biotechnol.*, 2005, **16**, 204-211.
30 B. W. Trautner, *Nat. Rev. Urol.*, 2012, **9**, 85-93.
31 A. I. Lopez, A. Kumar, M. R. Planas, Y. Li, T. V. Nguyen and C. Cai, *Biomaterials*, 2011, **32**, 4336-4346.
32 R. O. Darouiche, S. Riosa and R. A. Hull, *Infect. Control Hosp. Epidemiol.,* 2010, **31**, 659-661.
33 B. W. Trautner, A. I. Lopez, A. Kumar, D. M. Siddiq, K. S. Liao, Y. Li, D. J. Tweardy and C. Cai, *Nanomedicine: Nanotechnology, Biology and Medicine*, 2012, **8**, 261-270.
34 L. Ferrières, V. Hancock and P. Klemm, *FEMS Immunol.Med. Microbiol.*, 2007, **51**, 212-219.
35 B. W. Trautner, M. E. Cevallos, H. Li, S. Riosa, R. A. Hull, S. I. Hull, D. J. Tweardy and R. O. Darouiche, *J. Infect. Dis.*, 2008, **198**, 899-906.
36 P. Andersson, I. Engberg, G. Lidinjanson, K. Lincoln, R. Hull, S. Hull and C. Svanborg, *Infect. Immun.*, 1991, **59**, 2915-2921.
37 P. Klemm, V. Hancock and M. A. Schembri, *Infect. Immun.*, 2007, **75**, 3688-3695.
38 B. W. Trautner, R. A. Hull and R. O. Darouiche, *Urology*, 2003, **61**, 1059-1062.
39 R. O. Darouiche, B. G. Green, W. H. Donovan, D. Chen, M. Schwartz, J. Merritt, M. Mendez and R. A. Hull, *Urology*, 2011, **78**, 341-346.
40 G. Zhou, W. J. Mo, P. Sebbel, G. W. Min, T. A. Neubert, R. Glockshuber, X. R. Wu, T. T. Sun and X. P. Kong, *J. Cell Sci.*, 2001, **114**, 4095-4103.
41 J. Bouckaert, J. Mackenzie, J. L. de Paz, B. Chipwaza, D. Choudhury, A. Zavialov, K. Mannerstedt, J. Anderson, D. Pierard, L. Wyns, P. H. Seeberger, S. Oscarson, H. De Greve and S. D. Knight, *Mol. Microbiol.*, 2006, **61**, 1556-1568.
42 X. P. Qian, S. J. Metallo, I. S. Choi, H. K. Wu, M. N. Liang and G. M. Whitesides, *Anal. Chem.*, 2002, **74**, 1805-1810.
43 K. A. Barth, G. Coullerez, L. M. Nilsson, R. Castelli, P. H. Seeberger, V. Vogel and M. Textor, *Adv. Funct. Mater.*, 2008, **18**, 1459-1469.
44 P. Subramanian, F. Barka-Bouaifel, J. Bouckaert, N. Yamakawa, R. Boukherroub and S. Szunerits, *ACS Appl. Mater. Interfaces*, 2014, **6**, 5422-5431.
45 C. Beloin, A. Houry, M. Froment, J.-M. Ghigo and N. Henry, *PLoS. Biol.*, 2008, **6**, 1549-1558.

46 K. Otto, *PLoS. Biol.*, 2008, **6**, 1392-1394.
47 O. Habimana, A. J. C. Semião and E. Casey, *J. Membr. Sci.*, 2014, **454**, 82-96.
48 S. Andersson, G. K. Rajarao, C. J. Land and G. Dalhammar, *Fems Microbiol. Lett.*, 2008, **283**, 83-90.
49 D. J. Miller, P. A. Araújo, P. B. Correia, M. M. Ramsey, J. C. Kruithof, M. C. M. van Loosdrecht, B. D. Freeman, D. R. Paul, M. Whiteley and J. S. Vrouwenvelder, *Water Res.*, 2012, **46**, 3737-3753.
50 N. Cerca, G. B. Pier, M. Vilanova, R. Oliveira and J. Azeredo, *Res. Microbiol.*, 2005, **156**, 506-514.
51 P. Sommer, C. Martin-Rouas and E. Mettler, *Food Microbiol.*, 1999, **16**, 503-515.
52 G. Schmiemann, E. Kniehl, K. Gebhardt, M. M. Matejczyk and E. Hummers-Pradier, *Dtsch. Arztebl. Int.*, 2010, **107**, 361-369.
53 M. Graupe, T. Koini, V. Y. Wang, G. M. Nassif, R. Colorado, R. J. Villazana, H. Dong, Y. F. Miura, O. E. Shmakova and T. R. Lee, *J. Fluor. Chem.*, 1999, **93**, 107-115.
54 L. Shuang, P. Cao, R. Colorado, X. P. Yan, I. Wenzl, O. E. Shmakova, M. Graupe, T. R. Lee and S. S. Perry, *Langmuir*, 2005, **21**, 933-936.
55 J. Bouckaert, J. Berglund, M. Schembri, E. De Genst, L. Cools, M. Wuhrer, C. S. Hung, J. Pinkner, R. Slattegard, A. Zavialov, D. Choudhury, S. Langermann, S. J. Hultgren, L. Wyns, P. Klemm, S. Oscarson, S. D. Knight and H. De Greve, *Mol. Microbiol.*, 2005, **55**, 441-455.
56 M. Touaibia, A. Wellens, T. C. Shiao, Q. Wang, S. Sirois, J. Bouckaert and R. Roy, *Chemmedchem*, 2007, **2**, 1190-1201.
57 Z. F. Han, J. S. Pinkner, B. Ford, R. Obermann, W. Nolan, S. A. Wildman, D. Hobbs, T. Ellenberger, C. K. Cusumano, S. J. Hultgren and J. W. Janetka, *J. Med. Chem.,* 2010, **53**, 4779-4792.
58 M. Dhayal and D. A. Ratner, *Langmuir*, 2009, **25**, 2181-2187.
59 S. D. Knight and J. Bouckaert, in *Glycoscience and Microbial Adhesion*, 2009, vol. 288, pp. 67-107.
60 G. Qin, C. Santos, W. Zhang, Y. Li, A. Kumar, U. J. Erasquin, K. Liu, P. Muradov, B. W. Trautner and C. Cai, *J. Am. Chem. Soc.*, 2010, **132**, 16432-16441.
61 A. Bridier, F. Dubois-Brissonnet, A. Boubetra, V. Thomas and R. Briandet, *J. Microbiol. Methods*, 2010, **82**, 64-70.
62 B. W. Trautner, R. O. Darouiche, R. A. Hull, S. Hull and J. I. Thornby, *J. Urol., 2002, **167**, 375-379.*

Table of contents entry:
Mannoside-modified surfaces enhance the coverage and stability of benign biofilms leading to bacterial interference against pathogenic colonization for 11 days.

Keyword: bacterial interference, catheter-associated urinary tract infection, non-pathogenic bacteria, biofilms, silicone

Zhiling Zhu, Jun Wang, Analette I. Lopez, Fei Yu, Yongkai Huang, Amit Kumar, Siheng Li, Lijuan Zhang and Chengzhi Cai*

Surfaces Presenting α-Phenyl Mannoside Derivatives Enable Formation of Stable, High Coverage, Non-pathogenic *Escherichia coli* Biofilms against Pathogen Colonization